24

И Н С Т И Т У Т
ЯДЕРНОЙ ФИЗИКИ СОАН СССР

ПРЕПРИНТ И Я Ф 77 - 34

E.V. Shuryak

THEORY OF HADRONIC PLASMA

Новосибирск

1977

THEORY OF HADRONIC PLASMA

E.V.Shuryak

Abstract

For high enough density (or temperature) of matter the quarks, composing hadrons, are collectivized. The properties of such matter (hadronic plasma) are calculated in quantum cromodynamics as perturbational expansion in $\alpha_s = g^2/4\pi$, being small due to asymptotical freedom. Connection between antiscreening at small distances and screening at large ones in plasma is discussed. Comparison with earlier approaches based on hadronic gas picture allows to locate gas-plasma transition region. Some applications of the results are discussed: repulsive core of nucleons; stability of neutron stars; hot plasma, produced in hadronic collisions; and production rate of photons and dileptons by such plasma.

1. Introduction

If some matter is so dense that the separation of hadrons in it is smaller than their own size, they can not exist as separate objects and their constituents (quarks) are collectivized [1, 2]. In obvious analogy with electrons in condenced bodies we call such phase of matter the hadronic plasma. The analogy is even strengthened since we use the so called quantum cromodynamics (QCD) [3,4] as the underlying theory of strong interaction, which is in many aspects similar to quantum electrodynamics (QED). As it was noted in [2], due to asymptotical freedom of this theory, at asymptotically high density the equation of state is that of the ideal gas. The aim of the present work is to study the interaction in such matter and its effect on the thermodynamical quantities. Comparison of our results with calculations of low density phase (the hadronic gas) gives the location of gas-plasma transition. Note, that such transition is not strictly speaking the phase transition, in contrast to possible spontaneous symmetry breaking of weak interactions at $T \sim 300$ GeV [5].

The paper is organized as follows. Chapter 2 is devoted to notations of QCD, and brief discussion of its quantization in Coulomb gauge, most suitable for our problem. More place is given to derivation of the frequency summation method in the temperature Green function tecknique [6-8], which result in the sum of particle, antiparticle and virtual particle contributions in each diagram loop. In chpter 3 we show how antiscreening at small distances is changed to screening at large ones. Interesting cancellations of qluonic contribution in the static limit are found. In chapter 4 we calculate the ground state energy density for matter with high barion number density at zero temperature, refered below as "cold plasma" case. Arguments are given that results are resonable up to low transition densities $n_B \sim 2(F^{-3})$, although the parameter of the theory $\alpha_s = g^2/4\pi$ here is not small. Connection with repulsive core in nucleon-nucleon interaction is discussed. We found no place for stable configuration of

quark stars [9], and estimated the maximum neutron star mass to be 1.6÷2 Mo. The zero charge density and large temperature case ("hot plasma") is discussed in chapter 5. The transition temperature from gas to plasma is found to be 0.6 ÷ 0.8 GeV. Apart from cosmological applications such plasma is presumably produced in hadronic collisions [10, 11], so changes in equation of state may lead to observable effects. Chapter 7 is devoted to calculation of photon and lepton production rate by the hadronic plasma.

2. General theoretical remarks

The Lagrangian of quantum cromodynamics is

$$L = -\frac{1}{4} F^a_{\mu\nu} F^a_{\mu\nu} + \sum_N \bar{\psi}_N (i\partial_\mu \gamma_\mu + \frac{g}{2}\lambda^a \mathcal{B}^a_\mu \gamma_\mu - m_N)\psi_N \qquad (1)$$

where ψ_N corresponds to quarks of flawor N (namely u,d,s,c... quarks) the total number of flawors is N_f. The fields $\mathcal{B}^a_\mu$ corresponds to massless gauge fields-gluons, $a = 1...8$, λ^a is Gell-Mann matrices of SU(3), their indeces run over 1,2,3 and are omitted. Below we use their properties

$$Sp(\lambda^a \lambda^b) = 2\delta^{ab}; \quad [\lambda^a \lambda^b] = 2if^{abc}\lambda^c \qquad (2)$$

where f^{abc} is the structure constants of SU(3) normalized as

$$f^{abc} f^{abd} = 3\delta^{cd} \qquad (3)$$

Often some fictitions fields are added to (1), the so called Faddeev-Popov ghosts [12] in order to use covariant gauges. We do not use them, for the rest frame of the medium in any case fixes coordinates and this trick does not lead to simplifications. The Coulomb gauge is more convenient in this case [8], for it has only physical degrees of freedom. The quantization of gauge fields in such gauge has been given in [13]. Since Lagrangian (1) does not contain $\partial_0 \mathcal{B}^a_0$, the equation for $\mathcal{B}^a_0$ has no time derivatives, as in QED: $(m = 1,2,3)$

$$\Delta \mathcal{B}^a_0 = -gf^{abc}\mathcal{B}^b_m F^c_{0m} + \frac{g}{2}\sum_N \bar{\psi}_N \gamma_0 \lambda^a \psi_N \qquad (4)$$

But in contrast to QED, due to selfinteraction of gluons $\mathcal{B}^a_0$ can be expressed in terms of canonical variables $\mathcal{B}^a_m$, P^a_m only as infinite series in g. As a result, the Hamiltonian

$$H = \frac{1}{2}P^a_m P^a_m + \frac{1}{2}\partial_n \mathcal{B}^a_m \partial_n \mathcal{B}^a_m + gf^{abc}\partial_m \mathcal{B}^a_n \mathcal{B}^b_m \mathcal{B}^c_n + \frac{g^2}{4} f^{abc} f^{ade} \times$$

$$\times \mathcal{B}^b_m \mathcal{B}^c_n \mathcal{B}^d_m \mathcal{B}^e_n - \frac{1}{2}\mathcal{B}^a_0 \Delta \mathcal{B}^a_0 + \sum_N \bar{\psi}_N (i\partial_m \gamma_m + \frac{g}{2}\lambda^a \gamma_m \mathcal{B}^a_m + m_N - \frac{g}{2}\lambda^a \mathcal{B}^a_0 \gamma_0)\psi_N \qquad (5)$$

contains in fact infinite number of primary diagrams. This is not too bad for us since we do not discuss too high orders in g.

The renolmalizations of QCD are specific because of complicated and still unclear properties of this theory in infrared region, where the invariant charge grows [3]:

$$\alpha_s(q) = \alpha_s(m_0)/\left[1 + \left(\frac{11}{2} - \frac{N_f}{3}\right)\frac{\alpha_s(m_0)}{2\pi}\ln(q^2/m_0^2)\right] \qquad (6)$$

Here m_0 is some arbitrary normalization point. Let us fix m_0 by the condition

$$\alpha_s(m_0) = 1 \qquad (7)$$

The real value of m_0 is of interest because this parameter determines the applicability limits of our calculations, made by expantion in α_s. From the decay widths of φ and Ψ mesons [14], scaling violation in deep inelastic scattering [4,15], and MIT-bag fit to hadronic spectrum [16] one see that $m_0 = 0.2 \div 0.4$ GeV.

The calculations below are made by temperature Green function method [6-8]. We remind the reader that the only difference with the usual Feinmann rules is the change of all frequencies ω to discreate variables:

$$\omega \to \omega_n = \begin{cases} 2i\pi T n & \text{Bosons} \\ i\pi T(2n+1) & \text{Fermions} \end{cases}; \quad \int \frac{d\omega}{2\pi} \ldots \to \sum_n \qquad (8)$$

We shall use one standard summation method for (8). It can easily be transformed into contour integral [8]:

$$T\sum_n \Phi(\omega_n) = \frac{1}{2\pi i}\int_C dz\, f^{\pm}(z)\,\Phi(z) \qquad (9)$$

where $f_F^{\pm} = \pm\frac{i}{T}/(1+\exp(\mp zT))$ (Fermi statistics) and $f_B^{\pm} = \pm\frac{i}{T}/(\exp(\mp zT)-1)$ (Bose statistics) has poles in points (8) and contour C surrounds imaginary axis. Any $\Phi(z)$ can be written as $\Phi_+ + \Phi_-$ where $\Phi_+(z)$ has singularities in right half plane, and $\Phi_-(z)$ in the left one. If in the term with Φ_+ one chooses f^-, he can move the right part of the contour C to infinity, picking out singularities of $\Phi_+(z)$. If they are poles, it gives contributions of the type

$$\sum_i \operatorname{res}\Phi_+(z_i)\, f^-(z_i) \qquad (10)$$

As for the left half plane, one can substitute $f_F^- = 1 - f_F^+$ (for fermions) and the second term gives zero contribution. What remains is

$$\sum_i [\operatorname{res}\Phi_+(z_i) f^-(z_i) + \operatorname{res}\Phi_-(z_i) f^+(z_i)] + \int_{-i\infty}^{i\infty}\frac{dz}{2\pi i}\,\Phi(z) \qquad (11)$$

It is just the contribution of particles of the matter, anti-particles (holes), and virtual particles (radiative corrections). Note, that if one moves the integration contour in (11) to real axis, he obtains the usual $i\varepsilon$ prescription of Feinmann rules. Let us introduce special notation for the first two terms in (11), drowing new diagrams with δ-function Green function marked by lines with crosses. In hot plasma they correspond to

$$G^{(x)}(\varepsilon,p) = \frac{\hat p + m}{2\varepsilon}\,\frac{2\pi}{\exp(\varepsilon/T)+1}\,\delta(\varepsilon \pm \varepsilon_p) \qquad (12)$$

$$\mathcal{D}^{(x)\,ab}_{mn}(\varepsilon,K) = \frac{2\pi\,\delta(\omega^2-K^2)}{\exp(\omega/T)-1}\,\delta^{ab}(\delta^{mn}-K^mK^n/K^2)$$

for quarks, antiquarks and gluons, while for cold plasma case only quarks contribute:

$$G^{(x)}(\varepsilon,p) = \frac{\hat p + m}{2\varepsilon}\,2\pi\,\delta(\varepsilon-\varepsilon_p)\,\theta(\mu-\varepsilon_p) \qquad (13)$$

Finally, we may write the result of summation over frequencies in any loop as the sum of terms where one of the Green functions is with cross, plus one term without crosses. The usual integrals over frequencies is assumed in such notations.

3. Interaction in hadronic plasma

The question we are going to discuss is the following: whether interaction in medium increase with distance (anti-screening), as in vacuum; or is it screened? To give the answer one has to calculate temperature Green function of gluons

$$\mathcal{D}^{ab}_{\mu\nu}(x-y) = i\langle T(B^a_\mu(x), B^b_\nu(y))\rangle \qquad (14)$$

which in zero approximation in Coulomb gauge is

$$\overset{(0)}{\mathcal{D}}{}^{ab}_{mn}(\omega,K) = -\frac{\delta^{ab}(\delta^{mn}-K^mK^n/K^2)}{\omega^2-K^2}\;;\quad \overset{(0)}{\mathcal{D}}{}^{ab}_{00}(\omega,K) = -\frac{\delta^{ab}}{K^2} \qquad (15)$$

In general, there exist two transverse structures (instead of one polarization operator in vacuum) [8], Π_{00} and A:

$$\Pi_{mn}(\omega,K) = (\delta^{mn}-K^mK^n/K^2)A + \Pi_{00}K^mK^n\omega^2/K^4 \qquad (16)$$

Using (15,16) and Dyson equation one has the Green function of general form:

$$\mathcal{D}^{ab}_{mn}(\omega,K) = -\frac{\delta^{ab}(\delta^{mn}-K^mK^n/K^2)}{\omega^2-K^2-A}\;;\quad \mathcal{D}^{ab}_{00}(\omega,K) = -\frac{\delta^{ab}}{K^2\Pi_{00}} \qquad (17)$$

Diagrams of the order g^2 are shown at Fig.1 for $\Pi_{00}(\omega,K)$ (a-d) and for $A(\omega,K)$ (e-h) together with combinatorial factors.

Special discussion is needed for diagram Fig. 1(c), for Hamiltonian (5) does not contain such vertex. This term arizes because the interaction Hamiltonian through B^a_0 depends on canonical momenta $p^a_m = F^a_{0m}$. With the help of (4,5) one can write down the following expression for diagram (B):

$$\Pi^{(B)}_{00}(x-y) = \frac{g^2}{2}f^{abe}f^{ade}\langle T(\rho^b_m(x)B^c_m(x)\,\rho^d_n(y)B^e_n(y))\rangle \qquad (18)$$

Using Wick theorem we have two terms of the types $T(BB)\,T(pp)$ and $T(Bp)\,T(Bp)$. For their calculation one have to sub-

stitute $P^{(0)a}_m = \partial_0 B^a_m$ and express the result in terms of Green function $\mathcal{D}^{(0)}_{\mu\nu}$. Since time derivative does not commute with T-ordering, the additional term appears, which can be computed with the help of canonical commutator:

$$[B^a_m(x), P^b_n(y)]_{x_0=y_0} = i\delta^{ab}(\delta^{mn} - \partial_m\partial_n\Delta^{-1})\delta(\bar{x}-\bar{y}) \quad (19)$$

The nonzero result comes from $T(p,p)$ term and is exactly equal to that of diagram (c) contribution with vertex of the initial Lagrangian (1).

The next point is the summation over frequences. The "cross rule" of § 2 can be used and, since we have only one loop in this order, the result is just sum of the "vacuum" contribution $\Pi^{(v)}_{\mu\nu}$ without "crossed" Green function and the matter contribution $\Pi^{(m)}_{\mu\nu}$. Calculations of $\Pi^{(v)}_{\mu\nu}$ in Coulomb gange have been made in [13]. Note, that for Coulomb quanta vertexes are not renormalized and $\Pi^{(v)}_{00}$ gives directly the invariant charge (6). The logarithmic contributions of diagrams (d,b,a) is

$$\Pi^{(v)}_{00}(\omega,\kappa) = \frac{3g^2}{\pi^2}\left[-2\bar{K}^2 \ln\frac{\bar{K}^2}{m_0^2} + \frac{\bar{K}^2-\omega^2}{6}\ln\left(\frac{\bar{K}^2-\omega^2}{m_0^2}\right) + \frac{N_f(\bar{K}^2-\omega^2)}{9}\ln\left(\frac{\bar{K}^2-\omega^2}{m_0^2}\right)\right] \quad (20)$$

Note, the asymptotical freedom is due to diagram (d).

The $\Pi^{(m)}_{\mu\nu}$ contains no ultraviolet divergences because factors $f^{\pm}(\varepsilon)$ cut off momenta larger than T or chemical potential μ. Due to this, at large $q^2 \gg T^2, \mu^2$ (small distances) $\Pi^{(v)}_{\mu\nu}$ dominates.

The question we have to answer is the $\Pi_{\mu\nu}$ behaviour at large distances, or small $\omega,\kappa \ll T,\mu$. For hot plasma case due to descrete character of $\omega_n = 2\pi n T$ this region is reduced to the static case $\omega_n = 0$. Calculations of diagrams $(a-d)$, Fig.1, give for $\omega_n = 0$, $\kappa \to 0$

$$\Pi^{(m)}_{00} = \left(-\frac{N_f}{12} - \frac{1}{4} - \frac{1}{4} + \frac{1}{2}\right)g^2T^2 = -\frac{N_f g^2 T^2}{12} \quad (21)$$

Interesting, that gluonic part is canceled and quarks give

negative constant, that is usual screening. The diagrams $(e-f)$ give

$$A^{(m)}(\omega_n = 0, \kappa \to 0) = \left(0 - \frac{3}{4} + \frac{1}{4} + \frac{1}{2}\right)g^2T^2 = 0 + O(\kappa^2 \ln\frac{T^2}{\kappa^2}) \quad (22)$$

and therefore simple screening of "gluomagnetic" interaction is absent. Nevertheless, perturbation diagrams for thermodynamical quantities contain no infrared divergences due to additional power of $\bar{K}$ in "magnetic" vertexes. What is the result after summation of all diagrams for infrared region contribution is not yet known, although there are arguments that it is small by the ratio m_0/T.

For cold plasma infrared region is $\omega,\kappa \ll \mu$ and

$$\Pi^{(m)}_{00} = -\frac{g^2\mu^2 N_f}{4\pi^2}\left[1 - \frac{\omega}{2\kappa}\ln\left(\frac{\omega+\kappa}{\omega-\kappa}\right)\right] \quad (23)$$

and there is evident screening. The pole of Green function at $\omega_0^2 = g^2\mu^2 N_f/12\pi^2$ corresponds to longitudinal plasma oscillations. Diagrams with transverse gluons contains logarithmic divergence due to soft gluon emission, which are cut off by the imaginary part of $A^{(m)}$. The physical meaning of this is the finite radiation length in matter due to collisions.

4. Properties of cold plasma

Let us calculate the energy density of the matter with barion charge density so high that the corresponding chemical potential μ exceeds temperature and other chemical potentials, say corresponding to electric charge, strangeness etc. Zero approximation is the ideal quark gas [1,2] its energy density is

$$\mathcal{E}^{(0)}(\mu) = \sum_N \int \frac{6\,d^3p}{(2\pi)^3}\sqrt{p^2+m_N^2}\,\theta(\sqrt{p^2+m_N^2}-\mu) = \quad (24)$$

$$= \frac{3}{8\pi^2}\sum_N\left[p_N\mu(\mu^2+2p_N^2) - m_N^4\ln\left(\frac{p_N+\mu}{m_N}\right)\right]$$

where p_N is Fermi momentum of quarks of type N $p_N^2 = \mu^2 - m_N^2$ connected with their density by usual expression $n_N = p_N^3/\pi^2$ since the density of barionic

charge is $n_B = \frac{1}{3}\sum_N n_N$, (24) determines the needed dependence $\mathcal{E}^{(0)}(n_B)$. In reality, only for charmed quarks with $m_c \sim 1.5$ GeV its mass is essential, for others the ultrarelativistic formula

$$\mathcal{E}^{(0)}(\mu) = \frac{3\mu^4 N_f}{4\pi^2}\left(1 - \frac{1}{N_f \mu^2}\sum_N m_N^2\right) \qquad (25)$$

is sufficient. All corrections to be calculated below also correspond to this limit.

The Feinmann diagrams of the order g^2 are shown at Fig. 2 (a),(b). The first one is, in fact, equal to zero because of color indices. So, the "mean field" contribution appears only in the next orders. Therefore the main effect is the exchange energy (b).

According to "cross rule" of § 2, the sum over two frequencies gives contributions with 0, 1, 2 crosses. The first is power divergent and independent on the matter parameters, this is just the vacuum energy and must be rejected. The second is logarithmically divergent and corresponds to mass operator on the mass shell. For usual renormalization scheme it is zero par definition. But if we normalize Green functions in normalization point m_0, it is not zero. Since m_0 is rather small ($m_0 \simeq 0{,}2 \div 0{,}4$ GeV), for dense enough matter ($\mu \gg m_0$) this "effective mass" contribution is small compared to "interaction" term with two crosses:

$$\delta\Omega^{(2)} \approx -\int \frac{d^3p\, d^3k}{(2\pi)^6 4\varepsilon_p \varepsilon_k} \frac{g^2}{4} Sp(\lambda^a \lambda^a) = -\frac{\alpha_s N_f \mu^4}{2\pi^2} \qquad (26)$$

The same is true in higher orders, the number of "crosses" must be ≥ 2.

Contributions of the order g^4 are given by diagrams (c-f) of Fig. 2. Asymptotically largest is double log correction to backward scattering of quarks similar to that in QED [17]. This gives

$$\delta\Omega^{(d.l.)} = \delta\Omega^{(2)}\left(1 + \frac{\alpha_s}{3\pi}\ln^2\alpha_s\right) \qquad (27)$$

Note, that soft gluon emission gives double logs of infrared origin in diagrams (d-f) which are in fact exactly canceled in sum because only channels where charges do not change their direction contribute.

The next is the "mean" field" contribution of diagram (c). It has only one log, but N_f^2 instead of N_f. Low momentum transfer region is the main, so only Coulomb quanta are needed:

$$\delta\Omega^{(c)} = -\frac{1.4\,\alpha_s^2 N_f^2}{4\pi^3}\mu^4 \ln\alpha_s \qquad (28)$$

where 1.4 stands for numerical estimate of some integral.

Finally, about ultraviolet divergences. They all are charge renormalization and can be taken into account by the change of $\alpha_s(m_0)$ to $\alpha_s(\mu)$ (6) in the lower order expressions.

Taking all terms together one has

$$\Omega = -\frac{N_f \mu^4}{4\pi^2}\left[1 + \frac{2\alpha_s}{\pi} + \frac{2\alpha_s^2}{3\pi^2}\ln^2\alpha_s + \frac{1.4\alpha_s^2 N_f}{\pi}\ln\alpha_s + \dots\right] \qquad (29)$$

and the barion charge density is

$$n_B = -\frac{1}{3}\frac{\delta\Omega}{\delta\mu} \approx \frac{N_f \mu^3}{3\pi^2}\left[1 + \frac{2\alpha_s}{\pi} + \dots\right] \qquad (30)$$

Expressing μ through n_B one has the energy density $\mathcal{E}$

$$\mathcal{E} = \Omega + 3\mu n_B = \frac{9}{4} n_B^{4/3}\left(\frac{3\pi^2}{N_f}\right)^{1/3}\left[1 + \frac{2\alpha_s}{\pi} + \dots\right]^{-1/3} \qquad (31)$$

This dependence is compared to barion-hyperon gas model [18] in the lower part of Fig.3. Our results differ with those of [19] due to another sign of exchange correction (26) and the choice in [19] $\alpha_s = 2.2$ independent on momentum transfer. Note, that charm quark contribution is practically canceled by interaction decrease which makes the curves rather smooth. As a result, there exist no stable quark stars (see more detailed discussion of this in [9]). Another conclusion is that gravitational collapse of neutron stars takes place if its

mass $M \geq 1.6 \div 2\ M_\odot$ ($M_\odot$ is the Sun mass), see also discussion in [9, 19].

Where the asymptotics (31) becomes valid? Can it be used up to crossing point, at which quarks are presumably collectivized? If one looks at this formula (31) he answers "yes" for due to small coefficients corrections are rather small even for $\alpha_s \sim 1$. But it is clear that high order effects, which presumably make confinement of quarks, must come into play in this case. There are some arguments that such effects are due to terms of the type exp $(-\text{const}/\alpha_s)$. If so, the transition to asymptotics must be very rapid.

Other arguments in favour of this statement is provided by nuclear physics. It is known, that in the nucleon-nucleon interaction the repulsive component appears at internucleon distances $r_{NN} \sim 1$F and at $r_{NN} \sim 0.5$ F it is of the order of 1 GeV, the so called nucleon core. As it is noted in [20, 16] this phenomenon is naturally explained in QCD as Fermi repulsion of quarks with the same colors. Our calculations allows the more quantitative analysis. In the absence of strange quarks (the upper part of Fig.3) the curves of nucleon gas and hadronic plasma are crossed at $n_B = 1.5\ F^{-3}$ which indeed corresponds to $r_{NN} = 1$F where the potential turns. For $r_{NN} = 0.5$ F or $n_B = 10\ F^{-3}$ the ratio ε/n_B is really 1 GeV larger. This correspondence gives some hope that (31) is reasonable even at so low density. Note, that from this viewpoint the core in calculations [21, 22] is taken to be too hard, which was also noted in the discussion of the binding energies of finite nuclei, see e.g. [23].

5. Properties of hot plasma.

Now let us discuss the hot hadronic plasma, that is some matter with temperature T much larger than m_0 (7) and all chemical potentials. The zero approximation is the ideal gas of gluons, quarks and antiquarks. The corresponding energy density is

$$\overset{(0)}{\varepsilon}(T) = \int \frac{d^3p}{(2\pi)^3} \left[\frac{16p}{\exp(\frac{p}{T})-1} + \sum_N \frac{12\varepsilon_p}{\exp(\frac{\varepsilon_p}{T})+1} \right] \approx \tag{32}$$

$$\approx \frac{8\pi^2 T^4}{15} + \frac{7\pi^2 N_f T^4}{20}$$

The lower expression is the ultrarelativistic approximation, in general case integrals are calculated and tabulated in [10]. In astrophysical applications one must also account for photons and leptons, while in the hadronic collisions the system is too small and these particles come out freely.

For $\mu_i = 0$ the potential Ω coincides with free energy $F(T)$. The diagrams of the second order in g are shown at Fig. 4 together with combinatorial factors. As we have already discussed in § 3, only "two crosses" contribution must be taken into account, which can be written as

$$\delta F^{(2)} = -\int \frac{d^3p\, d^3k}{(2\pi)^6 4\varepsilon_k \varepsilon_p} \left\{ N_f f_F(\varepsilon_k) f_F(\varepsilon_p) \left(\frac{1}{2} M_{qq} + \frac{1}{2} M_{\bar{q}\bar{q}} + M_{q\bar{q}} \right) + \right. \tag{33}$$

$$\left. + N_f f_B(\varepsilon_k) f_F(\varepsilon_p) (M_{qB} + M_{\bar{q}B}) + \frac{1}{2} f_B(\varepsilon_k) f_B(\varepsilon_p) M_{BB} \right\}$$

where M_{qq}, $M_{\bar{q}\bar{q}}$ and $M_{q\bar{q}}$ is the amplitude of qq, $\bar{q}\bar{q}$ backward scattering and $q\bar{q}$ forward annihilation, given by diagram Fig. 5 (a); M_{qB} is that for qB scattering, Fig. 5 (b,c); and M_{BB} is the contribution of diagrams (d-f) for gluon-gluon scattering. In the ultrarelativistic case these amplitudes are significantly simplified

$$M_{qq} = -g^2 Sp(\lambda^a \lambda^a) \qquad M_{qB} = -2g^2 Sp(\lambda^a \lambda^a)$$

$$M_{BB} = 4g^2 (f^{abc} f^{abc}) \tag{34}$$

After the integration one has:

$$\delta F^{(2)} = \pi \alpha_s T^4 \left(-\frac{N_f}{6} + \frac{1}{3} \right). \tag{35}$$

In the next orders we come across some phenomenon, known already in usual plasma, namely the power infrared divergence. They are given by diagrams of Fig. 6 where dashed circles stands for Π_{00} . Really, the first one is

$$\delta F = -\frac{T}{4}\sum_n \int \frac{d^3K}{(2\pi)^3}\,\frac{\Pi_{00}^2(\omega_n,K)}{K^4} \qquad (36)$$

and since for $\omega_n = 0$, $K\to 0$ $\Pi_{00}\to$ const the integral diverges as dK/K^2 . The summation of all this set, as in usual plasma [24], gives the finite answer. This sum can be written as

$$\delta F_\Sigma = -T\int_0^g \frac{dg'}{g'}\sum_n \int \frac{d^3K}{(2\pi)^3}\,\frac{\Pi_{00}(K,\omega_n)}{K^2(K^2-\Pi_{00}(K,\omega_n))} \qquad (37)$$

where the integral over g' eliminate the combinatorial factor 1/n for n-th order. Note in this connection, that such trick in QED allows to express the thermodynamical quantities through Green function of photon or electron [7,8], while in QCD this is not possible due to variety of vertexes. But for the set of diagrams in question, this trick still works.

The contribution of small K and $n = 0$ in (37) can be easily found

$$\delta F_\Sigma \simeq \frac{T\Pi_{00}^3(0,0)}{6\pi} = -\frac{T^4}{6\pi}\left(\frac{\pi\alpha_s N_f}{3}\right)^{3/2} \qquad (38)$$

Note, that this term originate from distances of the order of $1/(gT)$, so the charge must be $\alpha_s(gT)$. We do not present here next corrections. The main are again double log terms, but even they are numerically small.

Finally one can take all this together and find the energy density

$$\mathcal{E} = F - T\frac{\partial F}{\partial T} = \frac{8\pi^2T^4}{15} + \frac{7\pi^2T^4N_f}{20} + \frac{\pi\alpha_s N_f T^4}{2} - \pi\alpha_s T^4 + \frac{T^4}{2\pi}\left(\frac{\pi\alpha_s N_f}{3}\right)^{3/2} \qquad (39)$$

At Fig.7 this dependence is shown as $\mathcal{E}/\mathcal{E}_0$, where $\mathcal{E}_0 = \pi^2T^4/30$ and is energy per one massless boson. So, our ratio is the effective number of degrees of freedom, e.g. the usual black body radiation in such units is just 2, the number of photon polarizations. The curve I corresponds to pion gas, curves 2, 3 corresponds to gas of all hadrons, stable or resonances [25]. The curves 4,5 corresponds to (39). The comparison shows that quarks are collectivized at $T_0 = 0.6 \div 0.8$ GeV. Let us note, that calculations [25] are based on the Beth-Ulenbeck method [26] valid if the gas parameter $n r_0^3$ is small. (n is particle density and r_0 the interaction radius). Since interaction of π, K is mainly due to ρ -mesons, the applicability limit of this model has been estimated in [25] to be $T_0 \sim m_\rho$ in nice agreement with T_0 value found above. In this connection we note, that the use of Beth-Ulenbeck method up to infinite density in the statistical bootstrap model [27] seems to be wrong, as well as the idea of limiting temperature, based on such treatment.

The change in the number of degrees of freedom from 3 at $T = 0.1$ GeV to ~50 at $T = 1$ Gev with necessity leads to $\mathcal{E}(T)$ dependence be stronger than T^4 (below T_0), probably $T^{6\div8}$ [25]. Another way to say this is the following: in this temperature region the square of the sound velocity $c^2 = dp/d\mathcal{E}$ (p is pressure) is not 1/3, as for ideal gas, but more likely $0.15 \div 0.2$ [25]. Interesting, that with this very equation of state the Landau theory of multiple production is in best agreement with data, see e.g. [11, 25, 28]. The predicted change in equation of state above T_0 to $\mathcal{E}\sim T^4$ or $c^2 = 1/3$ in the framework of this theory must result in observable effects, for example in slowing of the multiplicity growth with collision energy E_L for $E_L \gtrsim 10^3 \div 10^4$ GeV.

6. Production of photons and dileptons by hadronic plasma

Some time ago the so called prompt leptons ir hadronic coblisions have been discovered, that are those not due to π, K decays, see review [29]. Recently the prompt photons have alsc been seen [30]. Not discussing this phenomenon in details we just note, that these data can not be explained by known sources like bremstrahlung, vector meson decay, Drell-Yan mechanism [31] etc.

Long before these experiments E.L.Feinberg [32] has discussed this question in the framework of statistical approach to hadronic reactions. He proposed the mechanism for such particle production due to thermal fluctuations of charge and current in hadronic matter. The theory, discussed in the present work, is able to give estimates for such fluctuations.

The quantity we calculate is the production rate per unite time per unite volume dW/d^4x , given by the standard expression

$$dW/d^4x = (2\pi)^4 \delta^4(p_i - p_f) |\langle T_{if} \rangle|^2 \qquad (40)$$

The rules for its calculation is essentially the same as for energy density in § 5, but with imaginary part of Green functions of produced particles:

$$Im\, \mathcal{D}^{(\gamma)}_{\mu\nu}(q) = \pi \delta(q^2)(g_{\mu\nu} - q_\mu q_\nu / q^2)$$
$$Im\, \mathcal{D}^{(\gamma^*)}_{\mu\nu}(q) = \frac{\alpha}{3q^2}(g_{\mu\nu} - q_\mu q_\nu / q^2) \qquad (41)$$

Here γ^* stands for the pair of leptons with summation over their variables, except 4-momentum. We have also neglected the lepton mass compared to dilepton mass.

The dilepton production is possible in zero order in α_s and is given by diagram Fig. 8a, corresponding to $q\bar{q}$ anni-

hilation. The production rate is

$$\frac{dW^{\gamma^*}}{d^4x} \approx 3N_f \int \frac{d^3p_1 f_F(\varepsilon_1)}{(2\pi)^3 \cdot 2\varepsilon_1} \frac{d^3p_2 f_F(\varepsilon_2)}{(2\pi)^3 \cdot 2\varepsilon_2} Sp(\hat{P}_1 \gamma_\mu \hat{P}_2 \gamma_\nu) Im \mathcal{D}^{(\gamma^*)}_{\mu\nu}(P_1 + P_2) =$$
$$= \frac{\pi \alpha^2 N_f T^4}{144} \qquad (42)$$

The photon production is possible only due to strong interaction, otherwise $q\bar{q}$ pair can not be massless. The corresponding diagrams are shown at Fig.8 (b,c), their probability is

$$\frac{dW^{\gamma}}{d^4x} = \frac{e^2 q^2 N_f}{4} Sp(\lambda^a \lambda^a) \int \frac{d^3p_1\, d^3p_2\, d^3K}{8(2\pi)^9} \left[\frac{f_F(\varepsilon_1) f_F(-\varepsilon_2) f_B(K)}{\varepsilon_1 \varepsilon_2 K} + \right.$$
$$\left. + \frac{f_F(-\varepsilon_1) f_F(\varepsilon_2) f_B(K)}{\varepsilon_1 \varepsilon_2 K} + \frac{f_F(\varepsilon_1) f_F(\varepsilon_2) f_B(-K)}{\varepsilon_1 \varepsilon_2 (-K)} \right] \cdot |K T_{if}>|^2 \qquad (43)$$

Three terms in brackets correspond to processes $qB \to qB$; $\bar{q}B \to \bar{q}B$, $q\bar{q} \to B\gamma$. Note that $f_F(-\varepsilon) = 1 - f_F(\varepsilon)$ $f_B(-K) = -1 - f_B(K)$ and therefore factors in (43) for outgoing particles are correct. The square of matrix element T_{if} , summed over all indices, is given in ultrarelativistic case by diagram (b) only and equal to $8(p_2 \cdot K)/(p_1 \cdot K) + 8(p_1 \cdot K)/(p_2 K)$. Finally

$$\frac{dW^{\gamma}}{d^4x} = const \cdot \alpha_s \alpha N_f T^4 \qquad (44)$$

where constant is of the order of 10^{-1} and is determined by rather complicated integral. We have not computed it since in any case the comparison with data is resonable for differential spectra at high $p_\perp$ only. The absolute number of photons and e^+e^- is in any case given by soft photon emission of bremstrahlung origin. Such spectra can be calculated using (43, 42) and space-time dependence of T , for example, taken from the Landau theory.

In works [32] the production rate of photons and dilep-

tons has been estimated by dimensional arguments. Now we see that quite small numerical factors appears in the results. Note, that equilibrium fluctua tions we are discussing are in some sense the minimal ones, so we have estimated the effect from below. The further studies of these questions is , therefore, the measure of nonstatistical effects and are of greate interest.

Acknowledgements.

Author is indepted to A.I.Vainstein and I.B.Khriplovich for many useful discussions and to E.S.Fradkin for a helpful talk.

References

1. Ya.B.Zeldovich. Uspechi Fiz. Nauk 86, 303 (1965); Ya. B.Zeldovich, I.D.Novikov. Relativistic astrophysics. "Ńauka", 1967.
2. I.C.Collins, M.J.Perry. Phys.Rev.Lett. 34, 1353, 1975.
3. C.N.Yang, R.L.Mills. Phys.Rev. 96, 191, 1954; D.Gross, F.Wilczek. Phys.Rev.Lett. 26, 1343, 1973; H.D.Politzer, Phys.Rev.Lett. 26, 1346, 1973.
4. H.D.Politzer. Physics Reports 14, 130, 1974.
5. D.A.Kirzhnitz, A.D.Linde. Phys.Lett. 42B, 971, 1972.
6. T.Matsubara. Prog. Theor. Phys. 14, 351, 1955.
7. A.A.Abrikosov, L.P.Gorkov, I.E.Dzaloshinsky. "Methody Kvantovoj teorii polya v statisticheskoj fizike", Moskow, 1962.
8. E.S.Fradkin, Trudy FIAN (Lebedev Physical Institute) 29, 6, 1965.
9. U.H.Gerlach. Phys.Rev. 172, 172, 1968; N.Itoh. Progr. Theor.Phys. 44, 291, 1970; B.D.Keister, L.S.Kisslinger. Phys.Lett. 64B, 117, 1976.
10. L.D.Landau. Izvestia Akad.Nauk SSSR, ser.fiz. 17, 51, 1953; L.D.Landau, S.Z.Belenky. Uspekhi Fiz.Nauk 56, 309, 1955.
11. E.L.Feinberg. Physics Reports 5C, 237, 1972; E.V.Shuryak. Proceedings of 18-th International Conf. on High Energy Physics, Tbilisi, 1976.
12. L.D.Faddeev, V.N.Popov. Phys.Lett. 25B, 30, 1967.
13. I.B.Khriplovich. (Sov.J. of Nuclear Phys. Jaderinaya Fisika) 10, 409, 1969.
14. T.Appelquist, H.D.Politzer. Phys.Rev.Lett. 34, 43, 1975; A.De Rujula, S.L.Glashow. Phys.Rev.Lett. 34, 46, 1975.
15. A.I.Vainstein, V.I.Zaharov, V.A.Novikov, M.A.Shifman. Pisma JETP 24, 376, 1976.

16. A.Chodos et al. Phys.Rev. D9, 3471, 1974; D10, 2599, 1974; T. de Grand et al. Phys.Rev. D12, 2060, 1975.

17. V.G.Gorshkov, V.N.Gribov, L.N.Lipatov, G.B.Frolov. (Yadernaya Fisika, Sov. J. of Nucl. Phys.) 6, 129, 1967.

18. V.A.Ambartzumyan, G.S.Saakyan. Astronomicheskij Jurnal 37, 163, 1960.

19. G.Baym, S.A.Chin. Phys.Lett. 62B, 241, 1976.

20. L.L.Frankfurt, M.I.Strickman. X-th Winter school of Leningrad Nuclear Physics Institute, volume 2, p.449, 1975.

21. S.A.Chin, I.D.Walecka. Phys.Lett. 52B, 24, 1974.

22. V.R.Pandharipande. Nuclear Physics A178, 123, 1973.

23. J.W.Negele. Phys.Rev. C1, 1260, 1970.

24. M.Gell-Mann, K.Bruechner. Phys.Rev. 106, 364, 1957.

25. E.V.Shuryak. (Yadernaya Fisika Sov.J. of Nucl. Phys.) 16, 395, 1972; O.V.Zhirov, E.V.Shuryak. Sov.J. of Nucl.Phys. 21, 861, 1975.

26. E.Beth, G.E.Uhlenbeck. Physica 3, 729, 1936.

27. R.Hagedorn, J.Ranft. Nuovo Cim. Suppl. 6, 169, 1968.

28. B.Anderson, G.Jarlskog, C.Damgaard. Nuclear Physics B112. 413, 1976.

29. L.M.Lederman. Phys.Reports. 26C, N 4, 1976.

30. P.Darriulat et al. Report 341/A4-28 to 18 International High Evergy Physics Conf., Tbilisi, 1976.

31. S.D.Drell, T.M.Yan. Phys.Rev.Lett. 24, 181, 1970.

32. E.L.Feinberg. Izvestia Acad.Nauk SSSR, ser. fiz. 26, 622, 1962; Nuovo Cimento 34A, 391, 1976.

Figure Captions

1. Second order diagrams for Π_{00} (a-d) and Π_{mn} (e-h), solid lines means quarks; dashed and wavy ones are Coulomb and transverse gluons.
2. Diagrams for Ω potential of the cold hadronic plasma.
3. Energy density ratio to barion number density ε/n_B (GeV) versus n_B (F^{-3}) for cold hadronic plasma of zero isospin u,d quarks only (upper curves, left scale) and for all quarks (lower curves, right scale). The curves (a) and (f) corresponds to ideal gases of neutrons and neutrons with hyperons [18]; (b,g) and (c,h) to hadronic plasma with m_o= 0.2 and 0.4 GeV; (d) and (e) to nuclear matter calculations [21] and [22]. Arrows show the positions of nuclear density (n_o); strangeness (Σ^-) and charm (c) thresholds.
4. Second order diagrams for Ω potential of the hot hadronic plasma.
5. Diagrams, giving amplitudes M_{qq} (a); $M_{q\bar{q}}$ (b,c) and $M_{\bar{q}\bar{q}}$ (d-f), see (33,34).
6. Set of diagrams with power infrared divergences summed into (37,38).
7. Energy density ratio to $\varepsilon_o=\pi^2T^4/30$ (effective number of degrees of freedom) versus temperature T (GeV). Curve 1 is pion gas; 2,3 - all mesons and all particle gas 25; 4,5 is the hot plasma with m_o = 0.4 and 0.2 GeV.
8. Diagrams for dilepton (a) and photon (b,c) production rate. Dotted lines are γ and γ^*.

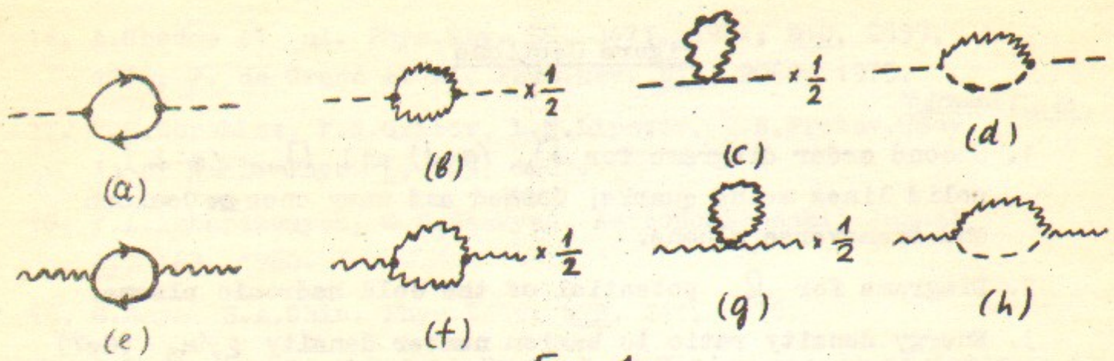

Fig. 1

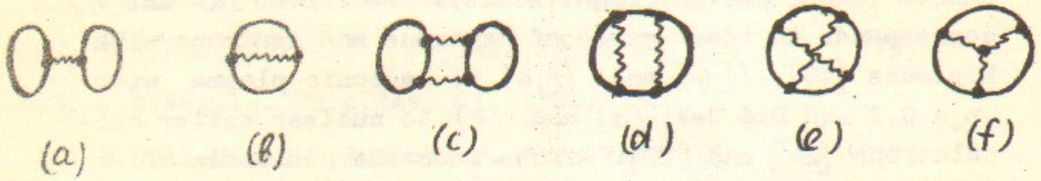

Fig. 2

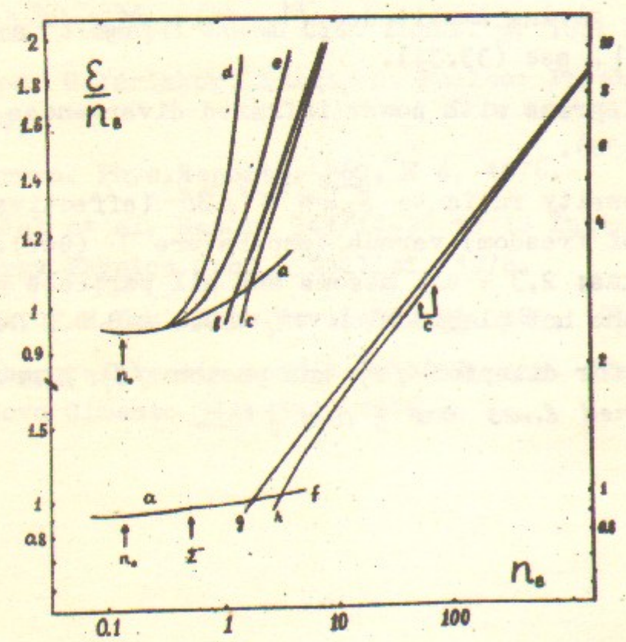

Fig. 3

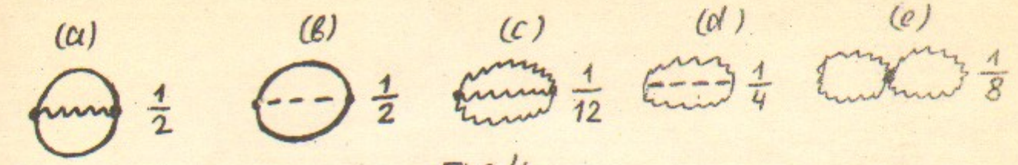

Fig 4

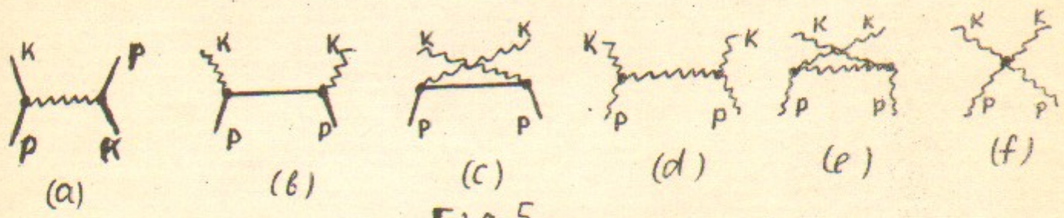

Fig.5

Fig.6

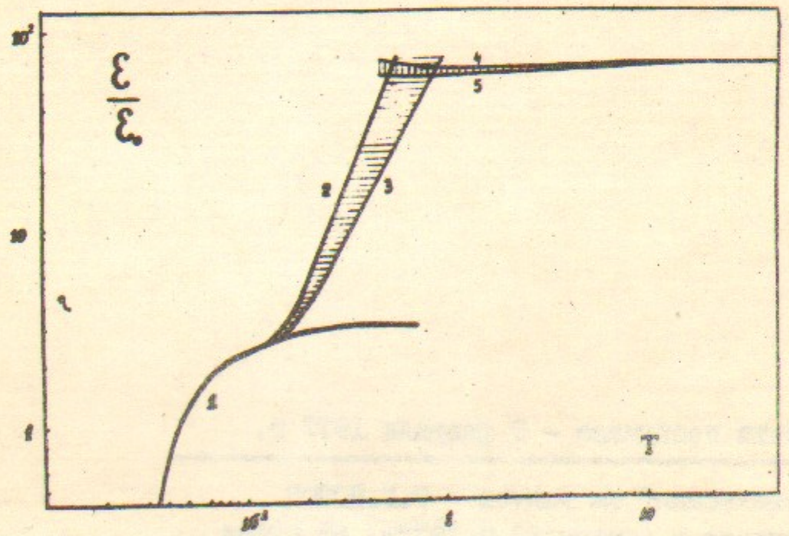

Fig.7

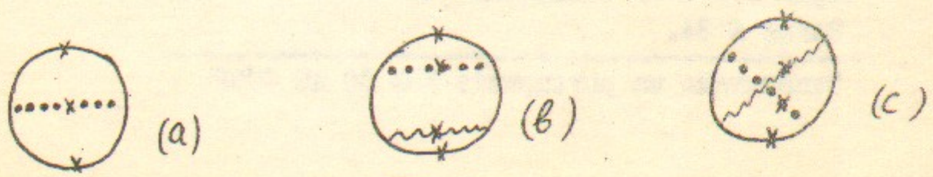

Fig 8

Работа поступила - 9 февраля 1977 г.

Ответственный за выпуск - С.Г.ПОПОВ
Подписано к печати 23.III-1977г. МН 02694
Усл. 1,7 печ.л., 1,4 учетно-изд.л.
Тираж 170 экз. Бесплатно
Заказ № 34.

Отпечатано на ротапринте ИЯФ СО АН СССР